

Original Article

Expression profiling of circular RNA reveals a potential miR-145-5p sponge function of circ-AFF2 and circ-ASAP1 in renal cell carcinoma

Ziliang Ji^{1*}, Ruijing Lu^{2*}, Tao Wu^{1*}, Zhong Chen¹, Zhiqiang Wen¹, Zhiguang Li¹, Xichun Zheng¹, Jinqi Tang¹, Xiangqiu Chen¹, Yinggui Yang¹, Qingyou Zheng¹

¹Department of Urology, Shenzhen Hospital of Southern Medical University, 1333 Xiniu Road, Shenzhen 518100, Guangdong, China; ²Department of Clinical Laboratory, Shenzhen Baoan Women's and Children's Hospital, Jinan University, 56 Yulv Road, Shenzhen 518133, Guangdong, China. *Equal contributors.

Received June 9, 2022; Accepted December 13, 2022; Epub January 15, 2023; Published January 30, 2023

Abstract: Objectives: Circular RNAs (circRNAs) are involved in carcinogenesis, though their expression profile in renal cell carcinoma (RCC) is uncharacterized. The tumor suppressor gene miR-145-5p is expressed in RCC tissues, but its relationship with circRNAs is unknown. Thus, we aimed to identify differentially expressed circRNAs in RCC tissues and to explore the interaction between these circRNAs and miR-145 in the development of RCC. Methods: We performed high-throughput sequencing and bioinformatics analyses to examine the expression pattern of circRNAs in RCC. Gene Ontology (GO) and Kyoto Encyclopedia of Genes and Genomes (KEGG) pathway analyses were used to functionally annotate differentially expressed circRNAs. Quantitative real-time polymerase chain reaction (qRT-PCR) was used for sequence verification. Small interfering RNAs were employed to investigate the function and mechanism of circRNAs in RCC. The relationship between miR-145-5p and circRNAs was confirmed using luciferase, RNA immunoprecipitation (RIP), and biotin-coupled probe RNA pull-down assays. Results: Fifty-three circRNAs were significantly and differentially expressed in RCC compared to normal control tissue. Bioinformatic analyses indicated that two significantly upregulated circRNAs, circ-AFF2 and circ-ASAP1, had sequences corresponding to miR-145 response elements. Consistently, the luciferase reporter, RIP, and biotin-coupled probe RNA pull-down assays showed that circ-AFF2 and circ-ASAP1 may repress miR-145 by acting as sponges. circ-AFF2 and circ-ASAP1 were highly expressed in RCC patient-derived tumor samples; their overexpression correlated with poor prognosis and low miR-145 levels. Knockdown of circ-AFF2 or circ-ASAP1 in RCC cell lines inhibited proliferation, underscoring their oncogenic function. A circRNA-miRNA network was constructed for RCC using the differentially expressed circRNAs and projected miRNAs. Candidate genes were verified by RT-qPCR and western blot, indicating that circ-AFF2 and circ-ASAP1 may be connected to RCC proliferation and metastasis. Conclusion: circ-AFF2 and circ-ASAP1 were upregulated in RCC and likely promote tumor progression by sponging miR-145. Therefore, both circRNAs should be investigated further as potential diagnostic and therapeutic targets for RCC.

Keywords: Circular RNA, circ-AFF2, circ-ASAP1, miR-145-5p, high-throughput sequencing, renal cell carcinoma

Introduction

Renal cell carcinoma (RCC) is the second most common urinary malignancy and it accounts for approximately 3% of all human carcinomas. An estimated 403,262 (2.2%) new cases of RCC were diagnosed and approximately 175,098 (1.8%) RCC-related deaths were recorded worldwide in 2018 [1]. Approximately 25-30% of RCC cases are in advanced stages at the time of diagnosis, and 30% of patients with localized tumors eventually proceed to meta-

static disease or experience post-surgery recurrence [2]. Although numerous molecular targeted therapies have shown promising results in clinical trials, the prognosis of patients with advanced-stage RCC remains poor. Therefore, there is an urgent need to further elucidate the underlying mechanisms of RCC and explore novel prognostic biomarkers and therapeutic targets.

circRNAs are noncoding RNAs that have an eponymous closed-loop structure [3] formed by

the covalent joining of the 3' and 5' ends. circRNAs are more stable than linear RNAs because they lack the 5'-cap and 3'-polyadenyl tail structure [3, 4]. circRNA sequences contain microRNA (miRNA) response elements (MREs) through which they act as miRNA sponges and relieve the inhibitory effect of the latter on target mRNAs [5]. Several circRNAs have recently been identified as tumor suppressors or oncogenes in several types of cancer, including prostate and breast [6, 7]. Thus, characterization of circRNA-mediated regulatory pathways can provide additional insight into cancer mechanisms and assist in identifying novel therapeutic targets and prognostic indicators.

miRNAs are small, noncoding endogenous RNAs of approximately 22 nucleotides (nt) in length that bind to target mRNAs and inhibit gene expression and translation [8]. Recent studies have indicated that miRNAs play a significant role in RCC progression [9]. For example, we previously demonstrated that miR-145-5p is significantly downregulated in RCC samples. Restoring miR-145-5p expression levels in RCC inhibited proliferation, migration, and invasion and enhanced apoptosis [10]. Recent evidence also indicates that miRNAs can be regulated by circRNAs [5].

In this study, the circRNA profiles of three RCC samples were analyzed via RNA sequencing (RNA-seq). circ-AFF2 and circ-ASAP1 were significantly upregulated in RCC tissues compared to normal renal samples. circ-AFF2 (hsa_circ_0001947-circBase ID) results from retro-splicing of AFF2 mRNA exon 3 on chromosome X: 47743428-147744289 and is 861 nt long. circ-ASAP1 (hsa_circ_0008934-circBase ID) results from the back-splicing of ASAP1 mRNA exons 9 to 14 on chromosome 8: 131164981-131193126 and is 550 nt long.

The biological roles of circ-AFF2 and circ-ASAP1 in RCC are largely unknown. We found that knocking down circ-AFF2 or circ-ASAP1 in RCC cell lines significantly inhibited their proliferation *in vitro*. Our molecular biology analyses further revealed that circ-AFF2 and circ-ASAP1 could act as miR-145 sponges in RCC cell lines. We constructed a circRNA-miRNA network to predict the potential functions of the RCC-related circRNAs and their interactions with miRNAs. The subsequent analysis revealed that knocking down circ-AFF2 and circ-ASAP1

diminished the expression of several genes involved in RCC growth and metastasis. Taken together, our data suggest that circ-AFF2 and circ-ASAP1 may act as oncogenes and could be used as novel RCC therapeutics.

Materials and methods

Tissue samples

This study was conducted following the approval of the ethical board of the Shenzhen Hospital of Southern Medical University (SZYEC2020-R001). All patients in this study provided written informed consent. Thirty-one pairs with histologically confirmed RCC (per World Health Organization criteria) and adjacent normal renal tissue specimens were obtained. All patients denied a history of chemotherapy, radiotherapy, or other cancers. Normal renal tissue was extracted from the edge of the tumors (>5 cm). Tumors were categorized following the Fuhrman system. All specimens were stored at -80°C until RNA extraction. **Table 1** summarizes the clinicopathological characteristics of the patients.

Cell culture

ACHN and 786-O renal cell carcinoma cell lines were purchased from American Type Culture Collection (ATCC, USA). Cells were cultured at 37°C under 5% CO₂ in RPMI medium (Gibco, Carlsbad, CA) and augmented with 10% fetal bovine serum (FBS).

RNA isolation and RNA-seq

Total RNA was extracted from frozen RCC samples using the TRIzol method (Life Technologies, Carlsbad, CA) and quantified using a NanoDrop spectrophotometer (Isogen Life Science). Samples with OD₂₆₀/OD₂₈₀ ratios from 1.8 to 2.1 were used for further analysis. Sequencing of RNA was carried out by Biotechnologies Genesky Inc. (Shanghai, China). Briefly, after eliminating ribosomal RNAs using an EpicentreRibo-zero™ rRNA Removal Kit (Epicentre Technologies, USA), the RNA libraries were built using NEBNext® Ultra™ as per the manufacturer's instructions. PCR was performed using Phusion High-Fidelity DNA Polymerase, Index (X) Primer, and Universal PCR primers. To evaluate the quality of the library, PCR products were purified and examined using Agilent software (Bioanalyzer 2100).

Table 1. Patient characteristics

Variable	Number of patients
Mean age (range), years	54 (24-70)
Sex (Male/Female)	20/11
Pathology	
Clear cell renal cell carcinoma	27
Renal cell carcinoma associated with Xp11.2 translocation/TFE3 gene fusion	2
Chromophobe renal cell carcinoma	2
Clinical Stage	
Stage I	27
Stage II	1
Stage III	2
Stage IV	1
Tumor Stage	
T1a	18
T1b	9
T2	1
T3	2
T4	1
Fuhrman grade	
G1	2 (T1a)
G2	16 (T1a), 9 (T1b), 1 (T3)
G3	1 (T2b), 1 (T3), 1 (T4)

circRNA identification

circRNAs were identified using bioinformatics programs including CIRI2 (v2.0.6), CIRCexplorer2 (v2.3.3), MapSplice (v.2.2.1), circRNA_finder (v.1.1), and find_circ (v.1.2). Gene annotation (GENCODE v. 19) and reference genome (GRCh37.p13 version) were downloaded from the GENCODE database. After assessing the quality of the RNA-seq data using FastQC and removing low-quality reads, clean reads were obtained and mapped to the reference genome using the designated reads aligner.

circRNA profiling analysis

The identified circRNAs were compared with those in circBase (140,790 human circRNAs) to screen for novel circRNAs. The number of junction reads (back-spliced) for each circRNA was extracted and combined to quantify the overlapping circRNAs. The abundance of the circRNAs was assessed and scaled to reads per million mapped reads. Package R (DESeq2) was employed to identify the circRNAs that were differentially expressed in RCC samples with ≥ 2 -fold changes; p -values ≤ 0.05 were considered statistically significant.

Gene ontology (GO) and Kyoto encyclopedia of genes and genomes (KEGG) analysis

The differentially expressed circRNAs were functionally annotated using KEGG (<http://www.genome.jp/kegg>) and GO (<http://www.geneontology.org>) analyses. GO terms related to biological process, cellular component, and molecular function were identified.

Quantitative real-time polymerase chain reaction (qRT-PCR)

Two upregulated circRNAs containing miR-145 response elements were further validated by qRT-PCR. Total RNA was extracted from 31 RCC tissue samples and adjacent normal renal tissue samples using TRIzol and reverse transcribed using random primers and a Reverse Transcriptase Kit, M-MLV (Life Technologies). qRT-PCR was performed using Ex Taq™ II SYBR® Premix (Takara, Tokyo, Japan) on a Real-Time PCR System (ABI 7500, Applied Biosystems, CA). GAPDH and small, U6 nuclear RNA were used as internal controls. Primers are presented in **Table 2**. Relative expression levels of the validated circRNAs are presented as $2^{-\Delta\Delta CT}$.

circ-AFF2 and circ-ASAP1 as potential miR-145-5p sponges in renal carcinoma

Table 2. qRT-PCR primers

Gene	circBase ID	Primer Type	Primer Sequence (5'-3')	Product length
circ-AFF2	hsa_circ_0001947	Forward	CCGACATCTCACCAACACT	164
		Reverse	GCATCACCTTTGTTTGTTC	
circ-ASAP1	hsa_circ_0008934	Forward	CATCTCACATGCCACATACA	102
		Reverse	CTTCCGCAATCTCAGCTCCT	
AFF2	/	Forward	GGACTTGGAGCAGCAGTG	184
		Reverse	AAGCGTGTCTGGACTCGG	
ASAP1	/	Forward	TGACTAGCAAACGCAGAACC	152
		Reverse	ACACACATTATATCCCCTCC	
GAPDH	/	Forward	AGAAGGCTGGGGCTCATTG	140
		Reverse	GCAGGAGGCATTGCTGATGAT	

RNase R treatment

RNA isolated from ACHN cells was treated for 30 minutes at 37°C with 3 U/mg RNase R (Geneseed Biotech, Guangzhou, China). qRT-PCR was used to assess the stability of circ-RNAs and their corresponding linear mRNAs.

Cell transfection and cell proliferation assays

Small interfering RNAs (siRNAs) targeting circ-AFF2 and circ-ASAP1 were obtained from Geneseed. The miR-145-5p mimic and antagonist were manufactured by RiboBio (Guangzhou, China). The siRNAs had the following sequences: si-circ-AFF2: CTCACATGCCACATACAAA and si-circ-ASAP1: TCACATGCCACATACAAA. RCC cells were transfected with the various constructs using Lipofectamine 3000 (Invitrogen, USA) as per the manufacturer's instructions. The effects of the siRNA and miRNA mimics were validated via qRT-PCR. A CCK-8 test was used to calculate RCC cell proliferation. Briefly, cells were cultured in 96-well plates for 24 hours before transfection; the CCK-8 reagent was added 0, 24, 48, and 72 hours after transfection. Absorbance was measured using a microplate reader (Bio-Rad).

Luciferase reporter assay

The amplified circ-AFF2 or circ-ASAP1 wild-type (WT) or mutant (Mut) sequences were inserted between the XhoI-NotI restriction sites in the luciferase vector (psiCHECK™-2, Promega, Madison, WI). The miR-145-5p and reporter plasmid were co-transfected into RCC cells. Luciferase activities were measured 48 h after transfection using a Dual-Luciferase Reporter Assay System (Promega).

RNA immunoprecipitation (RIP) assay

According to the manufacturer's instructions, RIP assays were performed using a Magna RIP RNA-binding protein immunoprecipitation kit (Merk-Millipore, Germany). After transfection with miR-145-5p mimics or the negative control, ACHN cells were lysed in RIP buffer. Cell lysates were treated at 4°C overnight with anti-Ago2 or IgG antibodies (Abcam, MA). qRT-PCR was then performed to measure the enrichment of circ-AFF2 and circ-ASAP1.

Biotin-coupled probe RNA pull-down assay

RiboBio produced biotin-labeled circ-AFF2 and circ-ASAP1 probes. The probe sequences were as follows: circ-AFF2: ATCACCTTTGTTTGTTC-ACTTGTGGAG; circ-ASAP1: TTCTCAATTTTT-GTATGTGGCATGTGAGATG; and negative control: GGGCGATCGGTGCGGGCCTCTTCGCTATTAC. ACHN cells were lysed and sonicated. Lysates were treated overnight at 4°C with streptavidin-coated magnetic beads (M-280, Invitrogen) and biotin-labeled probes. After washing the pull-down complexes, total RNA was extracted and purified using TRIzol.

Western blotting analysis

A BCA assay kit (Thermo Scientific, MA) was used to extract and quantify protein. After SDS-PAGE, equal amounts of protein were transferred to 0.22-m PVDF membranes at 250 mA for 120 minutes. Membranes were blocked with 5% BSA and treated overnight at 4°C with a primary antibody, followed by a secondary antibody. A Bio-Rad Chemical Doc XRS system was used to visualize the protein bands using an enhanced chemiluminescence kit (Millipore, Billerica, MA).

circ-AFF2 and circ-ASAP1 as potential miR-145-5p sponges in renal carcinoma

circRNA-miRNA-target gene network

The upregulated circRNAs containing putative miR-145 binding sites were screened using RegRNA2.0 (<http://regrna2.mbc.nctu.edu.tw>) [11], circRNA Interactome (<https://circinteractome.nia.nih.gov/>) [12], and StarBase (<http://starbase.sysu.edu.cn>) [13]. Targetscan (http://www.targetscan.org/vert_72) and MiRanda (<http://www.microrna.org/microrna/>) were used to predict the putative genes of the related miRNAs. The network of circRNA-miRNA target genes was constructed using Cytoscape software.

Statistical analysis

Paired and two-sided Wilcoxon rank-sum tests were used to compare differences between groups, and *p*-values with two-sided Wilcoxon rank-sum tests were used to compare the significance of differentially expressed circRNAs which were assessed using receiver operating characteristic (ROC) curves, and the area under the curve (AUC) was calculated to determine the diagnostic/significance value of these circRNAs in RCC. All figures were plotted using GraphPad Prism (v8.2.1).

Results

circRNA profiles in RCC and adjacent normal tissues

The circRNA expression profiles of RCC and adjacent normal tissues were obtained using RNA-seq. Tissue specimens from three clear cell RCC (ccRCC) patients (2 males and 1 female; average age: 49±5.56 years) were analyzed. A total of 2821 circRNAs were detected in the RCC tissues, of which 1072 were novel (**Figure 1A**). The majority of circRNAs in the RCC samples were exonic (89.68%), 4.96% were intronic, and 5.35% were intergenic (**Figure 1B**).

These circRNAs were distributed across all chromosomes, of which chromosome 2 harbored the highest number of circRNAs at 286. In contrast, the Y chromosome contained only three circRNAs, which was significantly fewer than the other chromosomes (**Figure 1C**). circRNA lengths ranged from 78 nt to 17,0452 nt with an average length of 3049 nt. Most circRNAs were 200-600 nt in length (45.23%, **Figure 1D**). Except for the 161 circRNAs of

unknown origin, the remaining 2660 circRNAs were derived from 1564 unique genes. Of these genes, 64.83% (1014/1564) generated only one circRNA, 18.93% (296/1564) generated two distinct circRNAs, 7.99% (125/1564) generated three circRNAs, and 8.25% generated four or more circRNAs (**Figure 1E**). The SLC26A7 gene produced the most distinct circRNAs with a total of 17.

Identification of differentially expressed circRNAs in RCC

RNA-seq analysis revealed a total of 4661 circRNAs, including 1504 in RCC tissues, 1840 in normal renal tissues, and 1317 in both tumor and non-tumor tissues (**Figure 1F**). Of the 1317 circRNAs present in both tissue types, 53 were differentially expressed between the tissue types; 21 were significantly over-expressed and 32 were under-expressed in the RCC tissues compared to the control renal tissues (*P*<0.05, fold-change >2.0) (**Figure 1G**). The top five over-expressed and under-expressed circRNAs in RCC are provided in **Table 3**.

GO and KEGG analysis of differentially expressed circRNAs

To determine the functional role of the parent genes of these differentially expressed circRNAs, we performed GO and KEGG analyses to identify their enriched molecular functions, cellular components, biological processes, and signaling pathways. The top ten enriched GO entries are shown in **Figure 2**. The top three enriched molecular functions were phosphatidylinositol binding (GO:0035091), tetrapyrrole binding (GO:0046906), and modified amino acid binding (GO:0072341) (**Figure 2A**). The most highly enriched cellular components were clathrin-coated pit (GO:0005905), apical plasma membrane (GO:0016324), and apical part of the cell (GO:0045177) (**Figure 2B**). The biological processes included response to organophosphorus (GO:0046683), response to cAMP (GO:0071320), regulation of sodium ion transport (GO:0002028), and cellular response to cAMP (GO:0071320), all of which were significantly enriched in the RCC tissues (**Figure 2C**). The top ten enriched pathways identified by KEGG analysis (**Figure 2D**) included olfactory transduction, cGMP-PKG signaling pathway, apelin signaling pathway, purine metabolism, parathyroid hormone synthesis secretion and

circ-AFF2 and circ-ASAP1 as potential miR-145-5p sponges in renal carcinoma

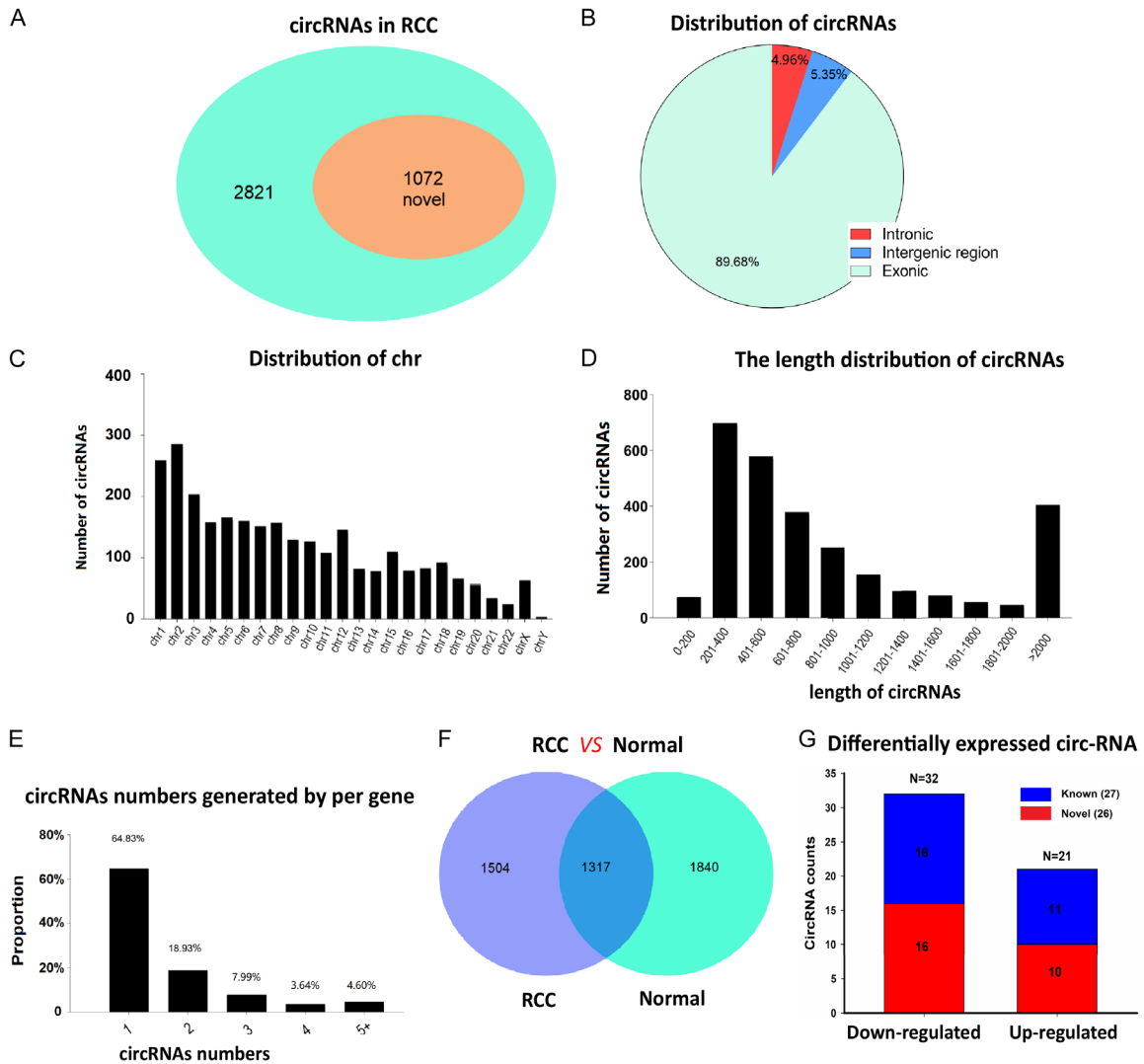


Figure 1. Circular RNA (circRNA) profile of renal cell carcinoma (RCC). A. The proportion of novel circRNAs among the identified circRNAs in RCC. B. Classification of circRNAs. C. Chromosomal distribution of circRNAs. D. circRNA length distribution. E. circRNA distribution per gene. F. Venn diagram illustrating differentially expressed circRNAs. G. Novel circRNA distribution in differentially expressed circRNAs.

action, glucagon signaling pathway, morphine addiction, renin secretion, cortisol synthesis and secretion, and ABC transporters.

Identification of circRNAs associated with miR-145-5p

Previously, we identified that miR-145 is expressed at lower levels in RCC samples than in control samples [10]. To identify the circRNAs that putatively bind to miR-145, we screened the StarBase, circRNA Interactome, and RegRNA2.0 databases to predict miRNA targets of differentially expressed circRNAs. Among the circRNAs expressed at higher levels in RCC tis-

sues, hsa_circ_0001947 (circ-AFF2) and hsa_circ_0008934 (circ-ASAP1) harbored sequences that perfectly matched the miR-145 response elements (Figures 3A and 4A).

Schematic illustrations of circ-AFF2 and circ-ASAP1 derived from the *AFF2* or *ASAP1* genes are shown in Figures 3B and 4B. The 861-bp pre-mRNA of *AFF2* contains only exon 3 and forms a closed loop that results in circ-AFF2. On the other hand, the pre-mRNA of *ASAP1* consists of six exons (14, 13, 12, 11, 10, and 9) and five introns (12, 11, 10, and 9), but circ-ASAP1 includes only the six exons and no introns. The GC content and evolutionary con-

Table 3. Top five over-expressed and under-expressed circRNAs in RCC

circRNA ID	circBase ID	Gene Name	Type	Predicted length	Adjusted p-value	Trend
1. chr15:57743698-57754090+	hsa_circ_0035435	CGNL1	exonic	600	0.0186	Down
2. chr6:51875107-51900519-	none	PKHD1	exonic	2654	0.0002	Down
3. chr1:59805630-59844509+	hsa_circ_0006633	FGGY	exonic	353	0.0316	Down
4. chr10:17024483-17061982-	none	CUBN	exonic	678	0.0014	Down
5. chr11:89088130-89135710-	hsa_circ_0023982	NOX4	exonic	588	0.0015	Down
6. chr1:16891302-16893846-	none	NBPF1	exonic	515	0.0007	Up
7. chrX:147743429-147744289+	hsa_circ_0001947	AFF2	exonic	861	0.0077	Up
8. chr13:78133939-78171724+	none	SCEL	exonic	636	0.00086	Up
9. chr12:6688012-6690515-	none	CHD4	exonic	261	0.0011	Up
10. chr9:103261047-103279053+	hsa_circ_0004425	TMEFF1	exonic	364	0.0490	Up

servation of the *AFF2* and *ASAP1* genes across 100 vertebrate genomes are shown in box 1 of **Figures 3B** and **4B**. The back-splice sites of the circRNAs were verified by Sanger sequencing (box 2, **Figures 3B** and **4B**). Furthermore, RNase R did not degrade circ-AFF2 or circ-ASAP1 though *AFF2* and *ASAP1* mRNA levels were significantly reduced after RNase R treatment (**Figure 5A** and **5B**). Thus, circ-AFF2 and circ-ASAP1 are circular and are more stable than linear mRNAs.

Knockdown of circ-AFF2 and circ-ASAP1 inhibits the proliferation of RCC cells in vitro

To determine the pathological role of circ-AFF2 and circ-ASAP1 in RCC, we synthesized specific siRNAs to target these circRNAs and verified their effectiveness by qRT-PCR. CCK-8 assays demonstrated the knockdown of circ-AFF2 or circ-ASAP1 in two RCC cell lines significantly decreased their proliferative rates (**Figure 5C** and **5D**).

The inhibition of cell proliferation by circ-AFF2 and circ-ASAP1 is reversed by knocking down miR-145

RCC cell lines were treated with a miR-145 inhibitor and transfected with si-circRNA vectors to determine if the proliferative effect of circ-AFF2 and circ-ASAP1 on RCC was dependent on miR-145. The CCK-8 experiment revealed that suppressing miR-145 partially counteracted the loss of cell viability induced by the downregulation of circ-AFF2 and circ-ASAP1 (**Figure 5E** and **5F**).

circ-AFF2 and circ-ASAP1 act as sponges for miR-145-5p

To further elucidate the interaction of circ-AFF2 and circ-ASAP1 with miR-145-5p, we cloned WT and Mut circ-AFF2 and circ-ASAP1 sequences into luciferase reporters. RCC cells were transfected with the respective constructs and a miR-145-5p mimic. Luciferase activity was repressed by overexpression of miR-145-5p in cells expressing WT circ-AFF2 and WT circ-ASAP1. However, this was not observed in cells expressing the mutant circRNAs (**Figure 6A** and **6B**). Furthermore, knockdown of circ-AFF2 and circ-ASAP1 significantly increased miR-145-5p levels in ACHN and 786-O cells (**Figure 6C**). The Ago-RIP tests revealed direct connections between miR-145 and circ-AFF2 and circ-ASAP1 (**Figure 6D**). Data from biotin-coupled probe pull-down tests indicated that overexpression of circ-AFF2 and circ-ASAP1 dramatically enriched miR-145 in RCC cells (**Figure 6E**). Taken together, circ-AFF2 and circ-ASAP1 function as miR-145-5p sponges in RCC.

The regulatory potential of circ-AFF2 and circ-ASAP1 in RCC

Using bioinformatics tools, we developed an interaction network of circRNA-miRNA-mRNA to examine the potential biological activities of circ-AFF2 and circ-ASAP1. The network includes 9 miRNAs and 42 mRNAs as illustrated in **Figure 7A**. Because circ-AFF2 and circ-ASAP1 are associated with RCC cell proliferation, we evaluated the expression of cell proliferation-related genes in the above network after circRNAs were knocked out. *ABCE1*, *SRGAP2*,

circ-AFF2 and circ-ASAP1 as potential miR-145-5p sponges in renal carcinoma

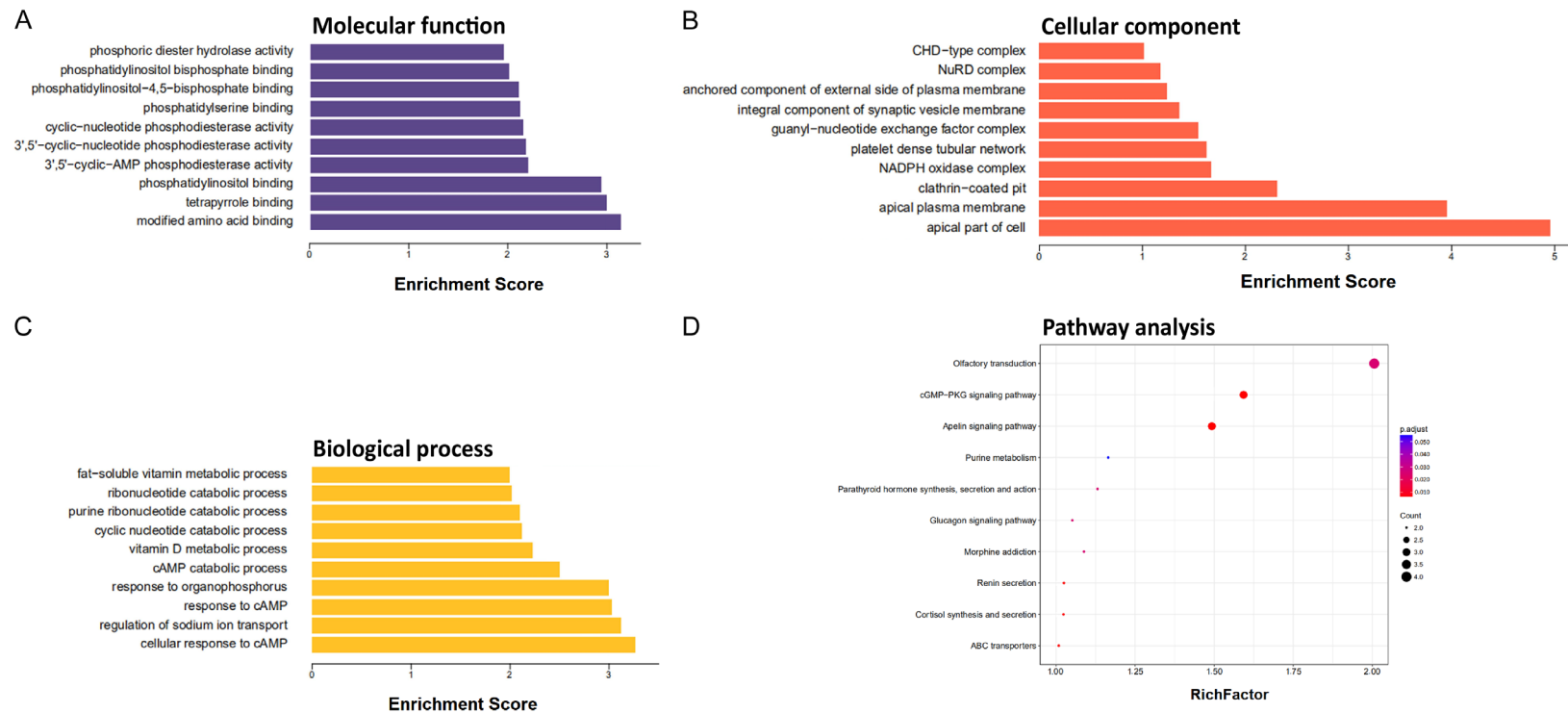


Figure 2. Gene Ontology (GO) and Kyoto Encyclopedia of Genes and Genomes (KEGG) pathway analyses of differentially expressed circRNAs. GO annotation of the differentially expressed circRNAs for (A) molecular function, (B) cellular components, and (C) biological process. The bar plots illustrate the top ten enriched terms of each category. (D) KEGG pathways of the differentially expressed circRNAs. The horizontal axis represents the RichFactor and the vertical axis represents the pathway name.

circ-AFF2 and circ-ASAP1 as potential miR-145-5p sponges in renal carcinoma

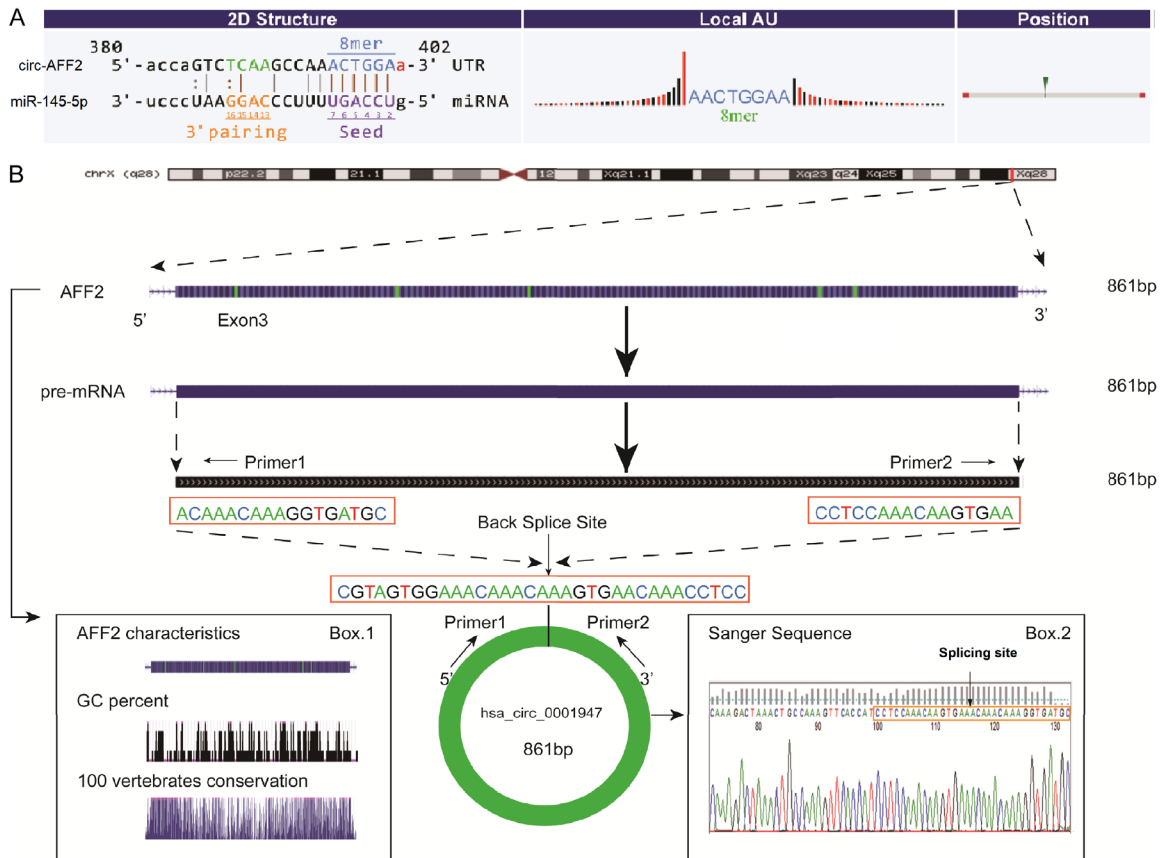


Figure 3. Characteristics and schematic illustration of circ-AFF2. A. Annotation of the predicted binding site sequence between circ-AFF2 and miR-145. The “2D Structure” column displays the binding sequence of circ-AFF2 and miR-145. The “Local AU” column shows the upstream and downstream sequences of the seed sequence consisting of 30 nucleotides. The “Position” column illustrates the possible position of miRNA response elements on the circRNA sequence. B. Characteristics and schematic illustration of circ-AFF2. Box 1-GC percentage and evolutionary conservation of AFF2 genes. Box 2-Specific back-splice site of circ-AFF2 as verified by Sanger sequencing.

FSCN1, VMP1, and HRNR expression levels were reduced after knockdown of circ-AFF2, whereas ABCE1, SRGAP2, FSCN1, and VMP1 expression levels were reduced after circ-ASAP1 knockdown (Figure 7B). As confirmation, we examined the regulation of these genes at the protein level using western blot assays. The protein levels of ABCE1, SRGAP2, and FSCN1 were similarly reduced in RCC cells with circ-AFF2 or circ-ASAP1 knocked out (Figure 7C).

Validation of circ-AFF2 and circ-ASAP1 expression levels in RCC tissues

To further verify the RNA-seq results, we measured the expression levels of circ-AFF2 and circ-ASAP1 in 31 pairs of RCC and adjacent normal renal tissue specimens by qRT-PCR. As shown in Figure 8A and 8B, circ-AFF2 and circ-

ASAP1 were more highly expressed in the RCC samples than in the control renal tissue samples ($P < 0.001$). Moreover, miR-145 was significantly downregulated in the RCC tissues compared to the control tissues (Figure 8C).

circ-AFF2 and circ-ASAP1 are potential biomarkers for RCC

We further evaluated the diagnostic value of circ-AFF2 and circ-ASAP1 for RCC by plotting ROC curves. circ-AFF2 had higher diagnostic accuracy than circ-ASAP1, with an AUC of 0.747 (95% CI: 0.624-0.871, $P < 0.001$, Figure 8D); the sensitivity was 0.742, the specificity was 0.677, and the cutoff value was 0.089. For circ-ASAP1, the AUC was 0.632 (95% CI: 0.492-0.771, $P = 0.0749$) with a cutoff value of 2.173, specificity of 0.871, and sensitivity of 0.419 (Figure 8E).

circ-AFF2 and circ-ASAP1 as potential miR-145-5p sponges in renal carcinoma

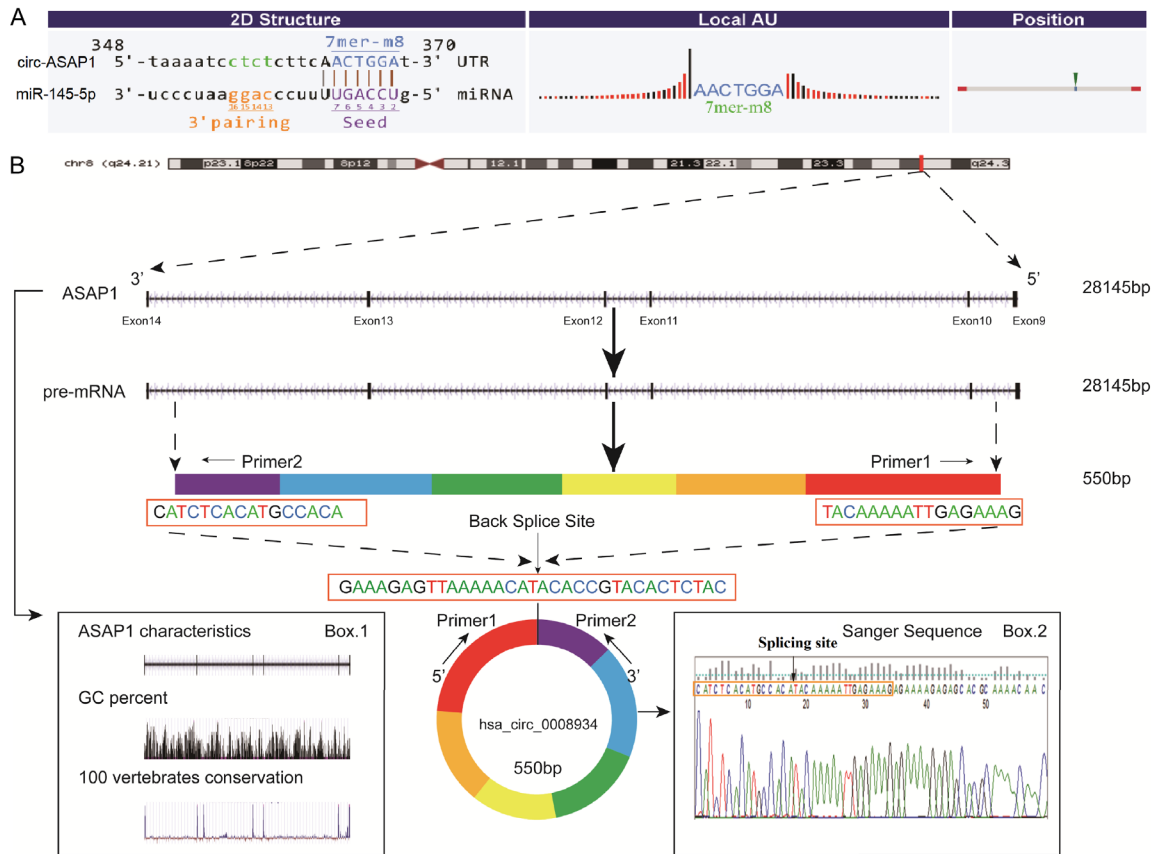


Figure 4. Characteristics and schematic illustration of circ-ASAP1. A. Annotation of the predicted binding site sequence between circ-ASAP1 and miR-145. B. Features and schematic illustration of circ-ASAP1. Box 1-GC percentage and evolutionary conservation of ASAP1 genes. Box 2-Specific back-splice site of circ-ASAP1 as verified by Sanger sequencing.

Discussion

Almost 98% of the human genome is transcribed into noncoding RNAs [14], including miRNAs, long noncoding RNAs (lncRNAs), small nuclear RNAs (snRNAs), and circRNAs, that are not translated into proteins. Recent high-throughput and bioinformatics techniques have uncovered several circRNAs that have potential roles and are expressed in multiple human malignancies, including RCC. Xue et al. established the circRNA expression profile of ccRCC through microarray analysis and found 53 over-expressed and 30 under-expressed circRNAs in ccRCC [15]. Another study used RNA-seq to identify 7335 differentially expressed circRNAs in RCC samples relative to control renal epithelial cells, including 1919 upregulated and 5416 downregulated circRNAs [14]. Here, we examined circRNA expression in RCC tissues and adjacent normal control tissues

and identified 2821 circRNAs in RCC tissues, including 1072 that were novel. The majority of these circRNAs are exonic, contain 200-600 nt, and are ubiquitous across all chromosomes, with chromosome 2 producing the most circRNAs. Furthermore, 21 significantly over-expressed and 32 under-expressed circRNAs were observed in RCC tissues.

circRNAs can regulate gene expression at multiple levels, including alternative splicing, miRNA maturation, transcription, RNA-protein binding, and translation. There is increasing interest in the “sponging” role of the circRNAs, in which they bind to specific miRNAs and relieve the inhibition of downstream target genes. By sponging miRNAs, circRNAs can regulate gene expression in cancer. For example, circ-AKT3 inhibits metastasis of ccRCC cells by altering the miR-296-3p/E-cadherin pathway [15]. Xiong et al. reported that circRNA-ZNF609

circ-AFF2 and circ-ASAP1 as potential miR-145-5p sponges in renal carcinoma

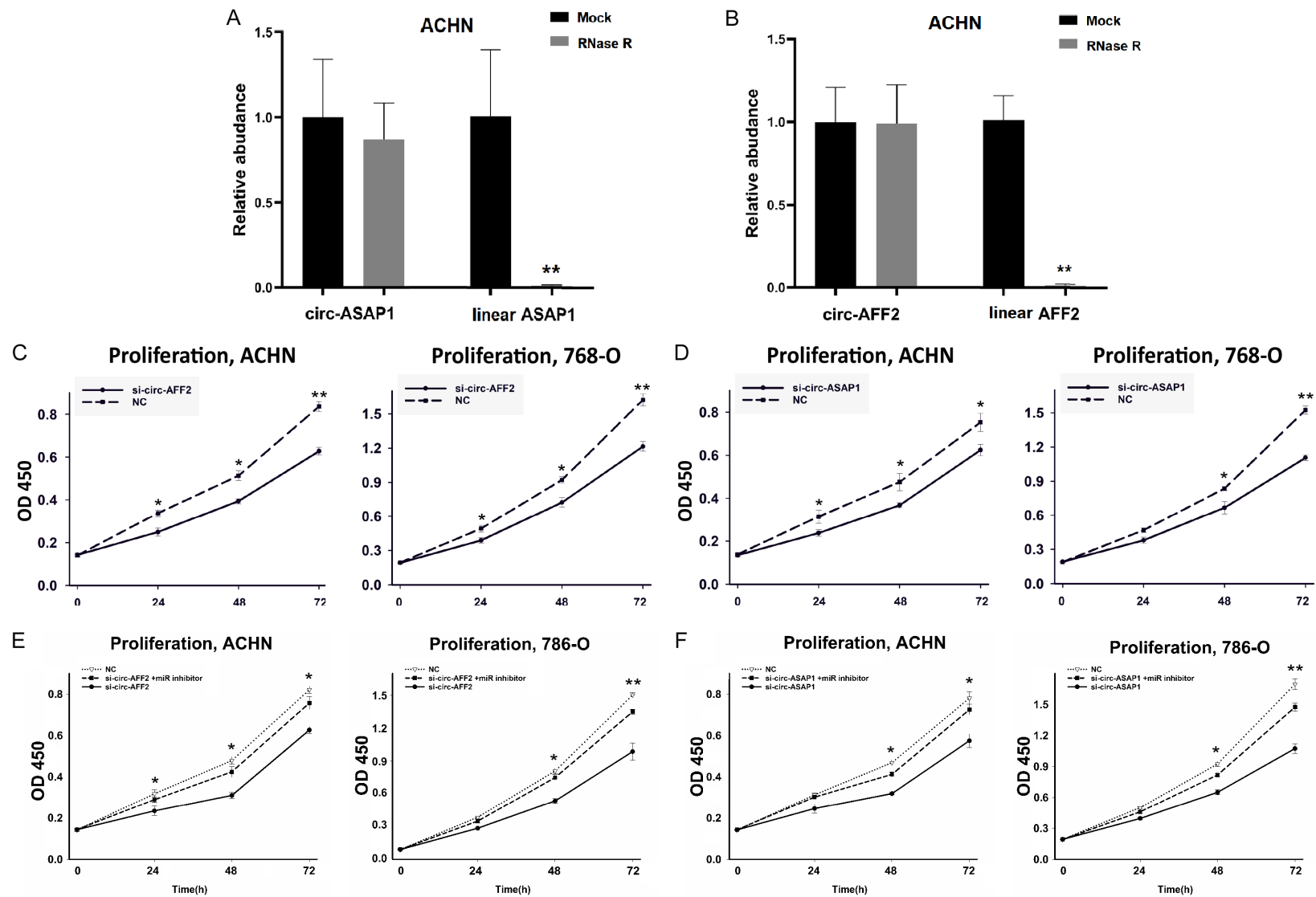


Figure 5. circ-AFF2 and circ-ASAP1 partially inhibit the proliferation of RCC cells in response to miR-145-5p. A, B. Relative expression levels of circ-AFF2, AFF2 mRNA, circ-ASAP1, and ASAP1 mRNA in ACHN cells after RNase R treatment. C, D. RCC cell growth patterns following transfection with si-circ-AFF2 or si-circ-ASAP1. E, F. RCC cell growth patterns after transfection with negative control (NC), si-circ, or si-circ+miR-inhibitor. * $P < 0.05$, ** $P < 0.001$.

circ-AFF2 and circ-ASAP1 as potential miR-145-5p sponges in renal carcinoma

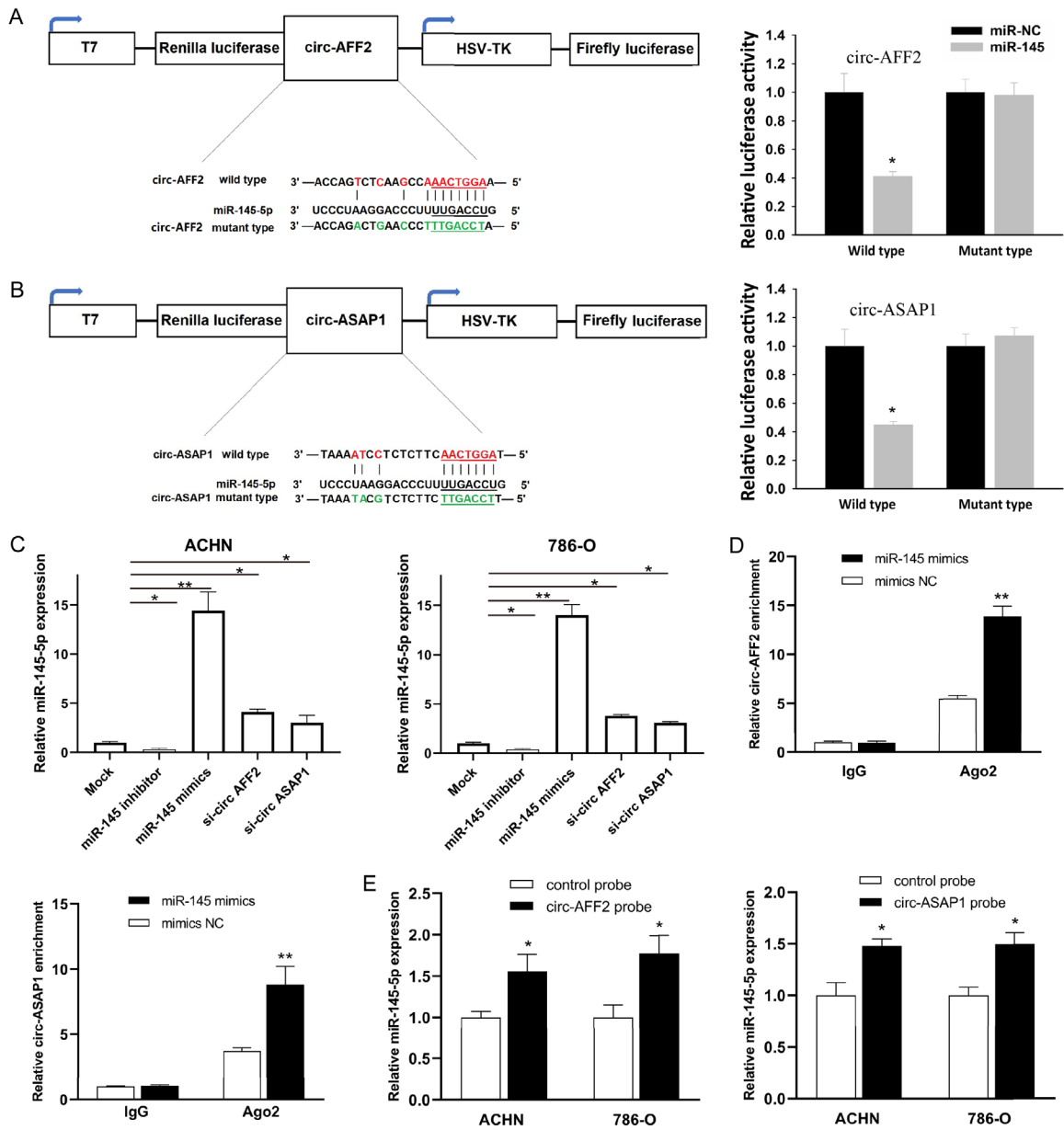


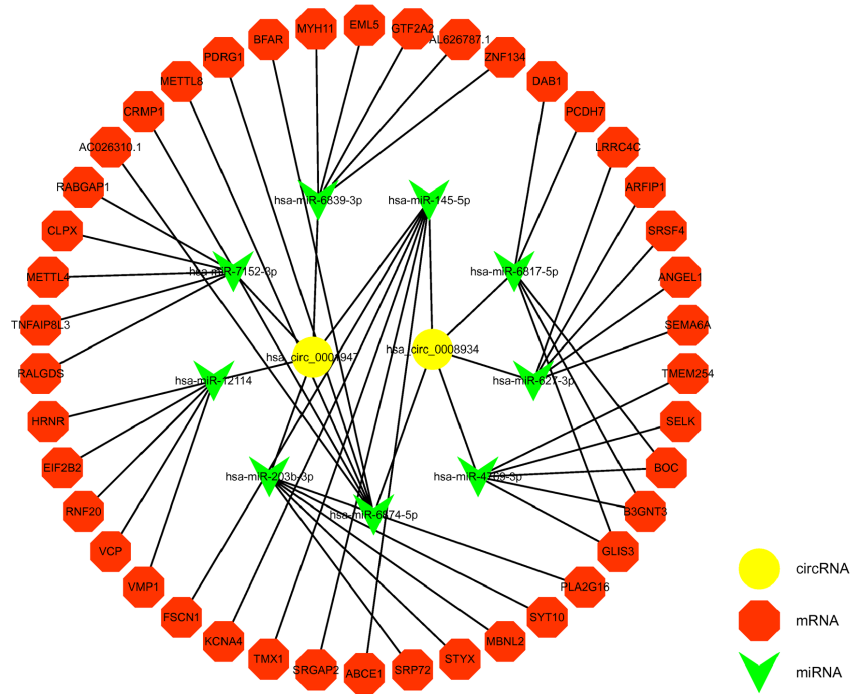
Figure 6. circ-AFF2 and circ-ASAP1 serve as sponges for miR-145-5p in RCC cell lines. **A.** Relative luciferase activity in RCC samples transfected with circ-AFF2-WT or circ-AFF2-Mut and miR-NC (control) or miR-145-5p mimic; wild-type and mutant sequences of the circ-AFF2 luciferase vectors. **B.** Relative luciferase activity in RCC samples transfected with circ-ASAP1-WT or circ-ASAP1-Mut and miR-NC or miR-145-5p mimic; wild-type and mutant sequences of the circ-ASAP1 luciferase vectors. **C.** Quantitative real-time polymerase chain reaction (qRT-PCR) was used to determine the expression levels of miR-145-5p in RCC cells after transfection with miR-145 mimics, miR-145 inhibitor, si-circ-AFF2, si-circ-ASAP1, or controls. **D.** After miR-145 mimics and NC mimics were transfected into ACHN cells, anti-Ago2 RNA immunoprecipitation (RIP) assays were performed to measure circ-AFF2 and circ-ASAP1 expression levels. **E.** Using circ-AFF2 or circ-ASAP1-specific probes, miR-145 was recovered. * $P < 0.05$, ** $P < 0.001$.

could increase the proliferation and aggressive capacity of RCC cells by upregulating FOXP4 by sponging miR-138-5p [16]. Likewise, circ-TLK1 also promotes the malignant potential of RCC cells by sponging miR-136-5p [14].

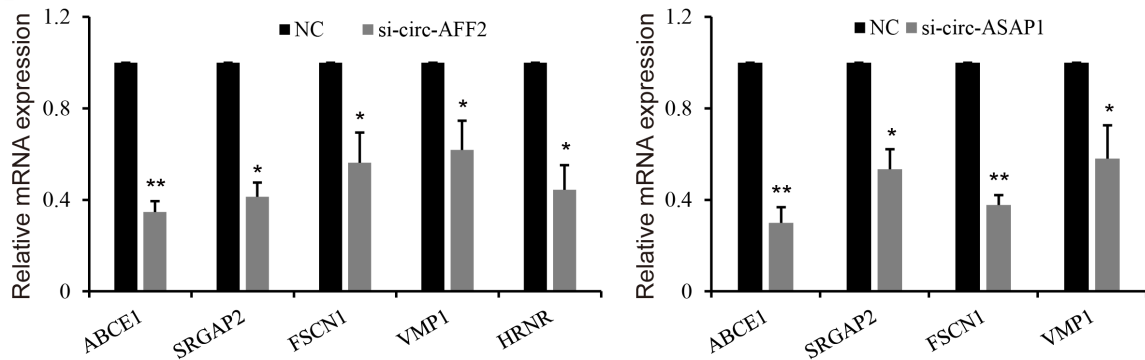
Since we previously demonstrated that miR-145 is a tumor suppressor in RCC, we screened for circRNAs with miR-145 response elements. circ-AFF2 and circ-ASAP1 were significantly upregulated in RCC tissues and harbored

circ-AFF2 and circ-ASAP1 as potential miR-145-5p sponges in renal carcinoma

A



B



C

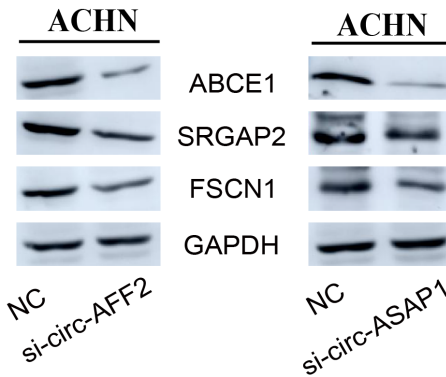
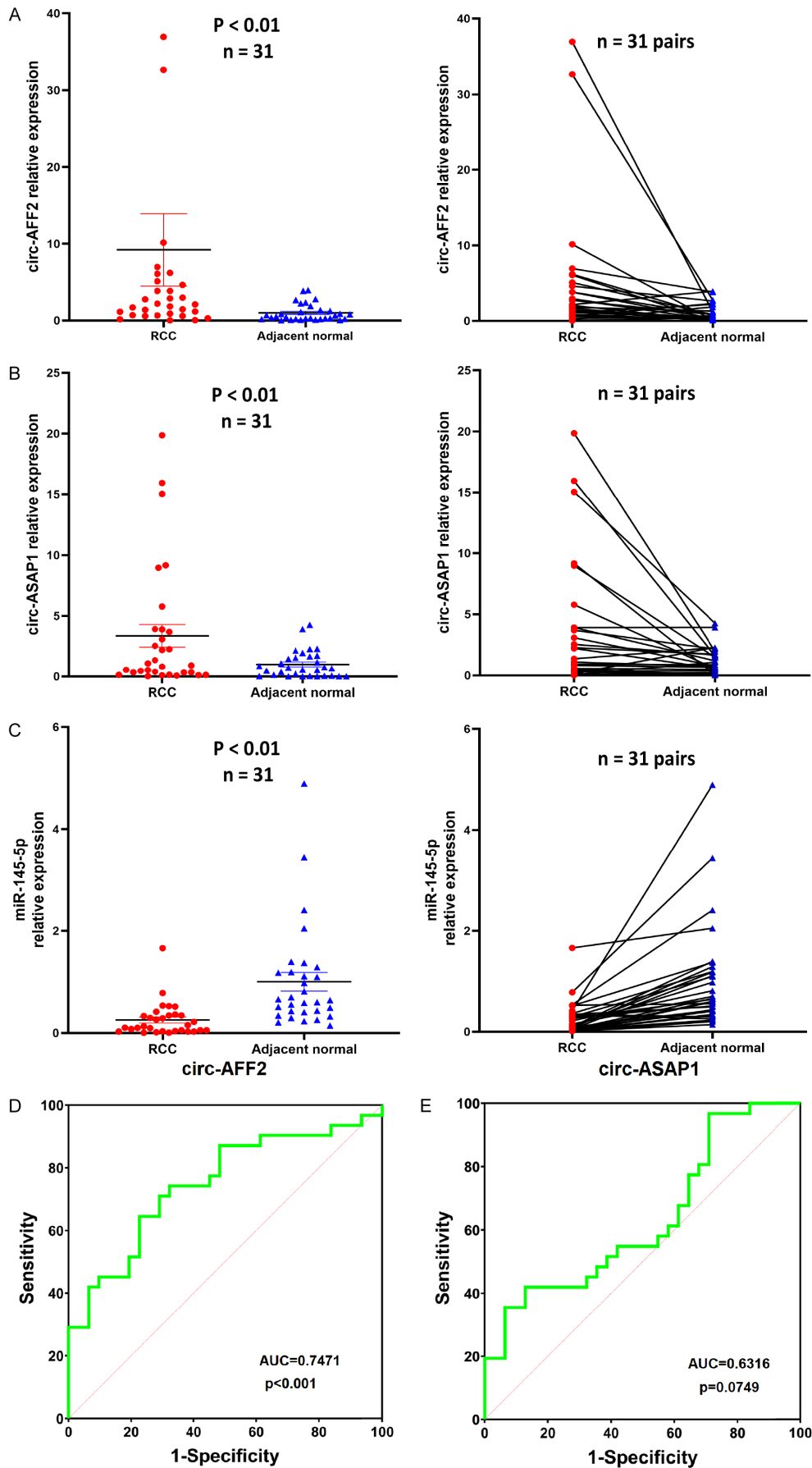


Figure 7. circ-AFF2 and circ-ASAP1 regulatory mechanisms in RCC. A. The circRNA-miRNA-mRNA interaction network. Both hsa_circ_0001947 (circ-AFF2) and hsa_circ_0008934 (circ-ASAP1) are represented by yellow circles. Green arrowheads represent the top nine miRNAs; target mRNAs are presented as red octagons. B. Various proliferation-related gene expression levels were examined by qRT-PCR in ACHN cells transfected with NC, si-circ-AFF2, or si-circ-ASAP1. C. Western blot analysis was used to determine the protein levels of *ABCE1*, *SRGAP2*, and *FSCN1* in ACHN cells transfected with NC, si-circ-AFF2, or si-circ-ASAP1. * $P < 0.05$, ** $P < 0.001$.

circ-AFF2 and circ-ASAP1 as potential miR-145-5p sponges in renal carcinoma



circ-AFF2 and circ-ASAP1 as potential miR-145-5p sponges in renal carcinoma

Figure 8. Clinical validation of circ-AFF2 and circ-ASAP1 in RCC specimens. Expression levels of circ-AFF2 (A), circ-ASAP1 (B), and miR-145 (C) in 31 RCC tissue samples relative to adjacent normal control samples. (D and E) The receiver operating characteristic (ROC) curve of circ-AFF2 (D) and circ-ASAP1 (E) in distinguishing RCC. AUC: Area under the Curve. * $P < 0.05$, ** $P < 0.001$.

sequences that bind to miR-145. circ-AFF2 exerts pro-tumorigenic effects in gastric cancer [17] and anti-tumorigenic effects in non-small cell lung cancer [18] by regulating different miRNAs. Li et al. demonstrated that circ-ASAP1 promotes the progression of liver cancer by modulating the axis of miR-1305/TMTC3 [19]. Another study showed that circ-ASAP1 increased the spread and migration of osteosarcoma cells by miR-145-5p sponging resulting in the overexpression of E2F3 [20].

circ-AFF2 and circ-ASAP1 expression levels in RCC were validated through qRT-PCR and were inversely related to miR-145 expression. Moreover, circ-AFF2 and circ-ASAP1 splicing sites and stability were verified using Sanger sequencing and RNase R treatment, respectively. *In vitro*, knockdown of circ-AFF2 and circ-ASAP1 decreased RCC cell proliferation, whereas knockdown of miR-145 mimicked the inhibitory effect of the circRNAs resulting in RCC cell proliferation. In addition, a dual-luciferase reporter test revealed that both circRNAs interact with miR-145-5p. RIP and RNA pull-down assays confirmed the miR-145 sponge function of circ-AFF2 and circ-ASAP1 in RCC.

We constructed a circRNA-miRNA-target gene network to explore possible mechanisms of circ-AFF2- and circ-ASAP1-induced RCC cell proliferation. Nine target miRNAs were identified including miR-145. mRNAs downstream of the nine miRNAs were also predicted. Follow-up experiments indicated that knocking down circ-AFF2 or circ-ASAP1 reduced the RNA and protein levels of the cell proliferation-related genes *ABCE1*, *SRGAP2*, and *FSCN1*. Therefore, circ-AFF2 and circ-ASAP1 may play a role in the formation of tumors and the development of RCC by sponging miR-145 resulting in overexpression of its downstream genes.

Because they are stable and resistant to degradation by RNases, circRNAs are promising biomarkers for many diseases, especially cancer, and the clinical relevance of several circRNAs has been reported in different carcinomas. For example, hsa_circ_0000190 is downregulated in both the tumor tissues and plasma of

patients with gastric cancer. In addition, hsa_circ_0000190 exhibits better sensitivity and specificity for diagnosing gastric cancer than CA19-9 and carcinoembryonic antigen (CEA) [21]. Li et al. found that high expression levels of circ-PDE8A in pancreatic tumors correlate significantly to T and TNM stages and lymphatic invasion. Furthermore, circ-PDE8A modulates the miR-338/MACC1/MET pathway in pancreatic cancer cells, resulting in increased migration, invasion, proliferation, and epithelial-mesenchymal transition (EMT) [22]. circPVT1 is similarly elevated in tumor tissues and sera of osteosarcoma patients and is associated with pulmonary metastasis, chemoresistance, and advanced Enneking stage. The AUC for circ-PVT1 in ROC analysis was 0.871, indicating its diagnostic potential in osteosarcoma [23]. Here, the AUC values of circ-AFF2 and circ-ASAP1 were 0.747 and 0.632, respectively. Thus, circ-AFF2 is a better diagnostic biomarker of RCC than circ-ASAP1.

In this study, we elucidated the circRNA profile of RCC and identified circ-AFF2 and circ-ASAP1 as potential oncogenes that function by sponging miR-145. In addition, both circRNAs are potential diagnostic biomarkers for RCC, which is consistent with previous reports on the diagnostic value of aberrantly expressed circRNAs. Our findings offer insights into circRNA-miRNA interactions in RCC, although the precise role of the circ-AFF2/circ-ASAP1/miR-145 axis in RCC development requires further study. Moreover, the molecular mechanisms and function of circ-AFF2 and circ-ASAP1 in RCC progression also warrant further investigation.

Acknowledgements

This research was funded by the National Nature Science Foundation of China (Grant No. 81902788), the "Miaomiao" cultivation project of Shenzhen Hospital Southern Medical University (Grant No. 2018MM07), the Baoan District of Shenzhen Basic Research Project (Grant No. 2020JD450), Natural Science Foundation of Guangdong Province (2020A-1515010902), and the Research Foundation of Shenzhen Hospital Southern Medical

University (Grant No. UN-KJ-KY200024-YYPT and Grant No. PT2020GZR07). We appreciate the language support MJ Language Editing Services (www.mjeditor.com) provided during this article preparation.

Disclosure of conflict of interest

None.

Address correspondence to: Ziliang Ji, Yinggui Yang and Qingyou Zheng, Department of Urology, Shenzhen Hospital, Southern Medical University, 1333 Xinhua Road, Shenzhen 518101, Guangdong, China. E-mail: jizl@foxmail.com (ZLJ); syyangyinggui@163.com (YGY); zhengqingyou@163.com (QYZ)

References

- [1] Bray F, Ferlay J, Soerjomataram I and Siegel RL. Global cancer statistics 2018: GLOBOCAN estimates of incidence and mortality worldwide for 36 cancers in 185 countries. *CA Cancer J Clin* 2018; 68: 394-424.
- [2] Choueiri TK and Motzer RJ. Systemic therapy for metastatic renal-cell carcinoma. *New Engl J Med* 2017; 376: 354-366.
- [3] Conn SJ, Pillman KA, Toubia J, Conn VM, Salmanidis M, Philips CA, Roslan S, Schreiber AW, Gregory PA and Goodall GJ. The RNA binding protein quaking regulates formation of circRNAs. *Cell* 2015; 160: 1125-1134.
- [4] Jeck WR, Sorrentino JA, Wang K, Slevin MK, Burd CE, Liu J, Marzluff WF and Sharpless NE. Circular RNAs are abundant, conserved, and associated with ALU repeats. *RNA* 2013; 19: 141-157.
- [5] Hansen TB, Jensen TI, Clausen BH, Bramsen JB, Finsen B, Damgaard CK and Kjems J. Natural RNA circles function as efficient microRNA sponges. *Nature* 2013; 495: 384-388.
- [6] Liang HF, Zhang XZ, Liu BG, Jia GT and Li WL. Circular RNA circ-ABCB10 promotes breast cancer proliferation and progression through sponging miR-1271. *Am J Cancer Res* 2017; 7: 1566-1576.
- [7] Huang C, Deng H, Wang Y, Jiang H and Zhao X. Circular RNA circABCC4 as the ceRNA of miR-1182 facilitates prostate cancer progression by promoting FOXP4 expression. *J Cell Mol Med* 2019; 23: 1-8.
- [8] Thomson DW and Dinger M. Endogenous microRNA sponges: evidence and controversy. *J Nat Rev Genet* 2016; 17: 272-283.
- [9] Lokeshwar SD, Talukder A, Yates TJ, Hennig MJP, Garcia-Roig M, Lahorewala SS, Mullani NN, Klaassen Z, Kava BR, Manoharan M, Soloway MS and Lokeshwar VB. Molecular characterization of renal cell carcinoma: a potential three-MicroRNA prognostic signature. *Cancer Epidem Biomar Prev* 2018; 27: 464-472.
- [10] Lu R, Ji Z, Li X, Zhai Q, Zhao C, Jiang Z, Zhang S, Nie L and Yu Z. miR-145 functions as tumor suppressor and targets two oncogenes, ANGPT2 and NEDD9, in renal cell carcinoma. *J Cancer Res Clin* 2014; 140: 387-397.
- [11] Chang TH, Huang HY, Hsu JB, Weng SL, Horng JT and Huang HD. An enhanced computational platform for investigating the roles of regulatory RNA and for identifying functional RNA motifs. *BMC Bioinformatics* 2013; 14 Suppl 2: S4.
- [12] Dudekula DB, Panda AC, Grammatikakis I, De S, Abdelmohsen K and Gorospe M. CircInteractome: a web tool for exploring circular RNAs and their interacting proteins and microRNAs. *RNA Biol* 2016; 13: 34-42.
- [13] Li JH, Liu S, Zhou H, Qu LH and Yang JH. starBase v2.0: decoding miRNA-ceRNA, miRNA-ncRNA and protein-RNA interaction networks from large-scale CLIP-Seq data. *Nucleic Acids Res* 2014; 42: D92-D97.
- [14] Li J, Huang C, Zou Y, Ye J, Jing Y and Gui Y. CircTLK1 promotes the proliferation and metastasis of renal cell carcinoma by sponging miR-136-5p. *Mol Cancer* 2020; 19: 103.
- [15] Xue D, Wang H, Chen Y, Shen D, Lu J, Wang M, Zebibula A, Xu L, Wu H, Li G and Xia L. Circ-AKT3 inhibits clear cell renal cell carcinoma metastasis via altering miR-296-3p/E-cadherin signals. *Mol Cancer* 2019; 18: 151.
- [16] Xiong Y, Zhang J and Song C. CircRNA ZNF609 functions as a competitive endogenous RNA to regulate FOXP4 expression by sponging miR-138-5p in renal carcinoma. *J Cell Physiol* 2019; 234: 10646-10654.
- [17] Bua X, Chen Z, Zhang A, Zhou X, Zhang X, Yuan H, Zhang Y, Yin C and Yang Y. Circular RNA circAFF2 accelerates gastric cancer development by activating miR-6894-5p and regulating ANTXR 1 expression. *Clin Res Hepatol Gastroenterol* 2021; 45: 101671.
- [18] Bao Y, Yu Y, Hong B, Lin Z, Qi G, Zhou J, Liu K and Zhang X. Hsa_Circ_0001947/MiR-661/DOK7 axis restrains non-small cell lung cancer development. *J Microbiol Biotechnol* 2021; 31: 1508-1518.
- [19] Li JX, Wang JJ, Deng ZF, Zheng H, Yang CM, Yuan Y, Yang C, Gu FF, Wu WQ, Qiao GL and Ma LJ. Circular RNA circ_0008934 promotes hepatocellular carcinoma growth and metastasis through modulating miR-1305/TMTC3 axis. *Human Cell* 2022; 35: 498-510.
- [20] Li S, Zeng M, Yang L, Tan J, Yang J, Guan H, Kuang M and Li J. Hsa_circ_0008934 promotes the proliferation and migration of osteosarcoma cells by targeting miR-145-5p to en-

circ-AFF2 and circ-ASAP1 as potential miR-145-5p sponges in renal carcinoma

- hance E2F3 expression. *Int J Biochem Cell Biol* 2020; 127: 105826.
- [21] Chen S, Li T, Zhao Q, Xiao B and Guo J. Using circular RNA hsa_circ_0000190 as a new biomarker in the diagnosis of gastric cancer. *Clin Chim Acta* 2017; 466: 167-171.
- [22] Li Z, Yanfang W, Li J, Jiang P, Peng T, Chen K, Zhao X, Zhang Y, Zhen P, Zhu J and Li X. Tumor-released exosomal circular RNA PDE8A promotes invasive growth via the miR-338/MACC1/MET pathway in pancreatic cancer. *Cancer Lett* 2018; 432: 237-250.
- [23] Kun-Peng Z, Xiao-Long M and Chun-Lin Z. Over-expressed circPVT1, a potential new circular RNA biomarker, contributes to doxorubicin and cisplatin resistance of osteosarcoma cells by regulating ABCB1. *Int J Biol Sci* 2018; 14: 321-330.